A Stand Alone Hybrid Power Generation System by MPPT Control Based on Neural Networks

N.Prakash[1], R. Ravikumar[2], I.Gnanambal[3]

[1]Department of EEE, Adhiyamaan College of Engineering, Hosur, India
pvl1517@gmail.com

[2]Department of EEE, Adhiyamaan College of Engineering, Hosur, India
rangan.ravi@gmail.com

[3]Department of EEE, Government College of Engineering, Salem, India
ignan1960@gmail.com

Abstract: *Hybrid Power Generation system with neural networks is proposed in this paper. The system consists of Wind Power, Solar power, Diesel Engine and an Intellectual controller. MATLAB2009b/Simulink was used to build the dynamic model and simulate the system. Here Maximum Power Point Tracking (MPPT) control is attained by Intellectual controller. It consists of Radial Bias Function Network (RBFN) and Modified Elman Neural Network (MENN). The pitch angle of wind turbine is controlled by the MENN and the solar system uses RBFN, where the output signal is used to control the dc/dc boost converters to achieve the MPPT. A Modified ENN and RBFN is used to control MPPT and to reduce the Total Harmonic Distortion (THD) in the Grid.*

Keywords: Modified Elman Neural Network, Radial Bias Function Network, MPPT, Total Harmonic Distortion

1. Introduction

In recent years, the development of Wind Energy Generation has been associated with wind farms located onshore and offshore. Variable-Speed wind turbines have many advantages. The wind farms are connected to strong transmission grids and their power ranges from some tens to a hundred megawatts [1].

Wind turbines can operate with Maximum Aerodynamic Efficiency, and the power fluctuations can be absorbed as an inertial energy in the blades [2]. In some applications, the wind turbine may be augmented by an additional source, and usually a Diesel Generator. These systems are called Wind–Diesel systems [1, 2] and they may be used to supply electrical energy to stand-alone loads, e.g., small villages that are not connected to the main utility. Most Diesel Generation systems operate at a constant rotational speed due to the restriction of constant frequency at the Generator terminals. However, Diesel engines have high fuel consumption when operating at light loads and constant speed [3]. More-over, for light loads at rated speed operation, not all the fuel is burned by the engine and wet stacking is produced. This increases maintenance costs [4]. In order to improve the efficiency and avoid wet stacking, a minimum load of about 30% to 40% is usually recommended by the manufacturers.

Applications with Photovoltaic (PV) energy and wind energy have been increased significantly due to the rapid growth of power electronics techniques [5]. The maximum power point of photovoltaic (PV) array is variational, so a search algorithm is needed according to the current–voltage (I–V) and power–voltage (P–V) characteristics of the solar cell. The perturbation and observation (P&O) MPPT algorithm is commonly used, due to its ease of implementation. It is based on the observation that if the operating voltage of the PV array is perturbed in a given direction and the power drawn from the PV array increases, which means that the operating point is moving toward the MPP, so the operating voltage must be further perturbed in the same direction. Otherwise, with the operating point moving away from the MPP, the direction of the operating voltage perturbation must be reversed. By using the P&O method, impedance matching is conducted between a boost converter and PV array in order to realize the MPPT function [6], [7].

The combination of battery energy storage, wind generating system and PV array in distributed power system can provide the effective, reliable, and durable power system. The system also provides energy saving and un-interruptible power within distribution network [8]. The parallel processing of wind energy generating system, PV system and battery storage will enhance the power flow in the distributed network. The wind energy generating system and PV system are used to charge the battery as and when the wind and solar power is available. The control method for the state of charge of battery unit was proposed in [9, 10]. The battery storage provides a rapid response for either charging/discharging the battery and also acts as a constant voltage source for the critical load in the distributed network. Novel two layer constant control scheme for a wind farm equipped with Doubly Fed Induction Generator (DFIG), each DFIG equipped with Energy Storage System (ESS) to generate desired amount of active power, where deviation between the available wind energy input and desired active power output compensated by ESS in [11]

Prakash et al [12], proposed a small Wind-diesel power generation system with neural network control for power quality improvement and maximum wind-power extraction. The mechanical power of the wind turbine can

be well tracked for both the dynamic and steady state, but the power deviation and speed tracking errors are large for transient response lasting for almost 20 secs.

Muljadi et al [13] developed pitch control and generator load control methods to adjust the aerodynamic power, but power coefficient C_p deviation is too large [13]. In order to improve the ability of identifying high-order systems, some modified ENN have been proposed recently, which proved to have more advantages than the basic ENN, including a better performance, higher accuracy, dynamic robustness, and a fast transient performance.

The Elman neural network (ENN) is a partial recurrent network model first proposed by Elman [14] which is a superior network. The ENN does not need to use the state as input or training signal, which makes the ENN superior to static feed-forward network and is used in dynamic system identifications widely [15].

An RBFN is used to adaptively compensate for the plant nonlinearities. It has a faster convergence property than common multiplayer-perceptron NN, but with a simpler network structure. RBFN also has a similar feature as the fuzzy-logic system, where the output value is calculated using the weighted-sum method, and the number of nodes in the hidden layer is the same as that of the "if–then" rules of the fuzzy system. With advantages of multiple facets and the self-adapting capabilities, RBFN is very useful for controlling nonlinear and time-varying dynamic systems where uncertainties and parameter variations need extra attention [16].

2. System Description

Recently, the growth of Wind and PV power generation system has exceeded the most optimistic estimation [15]. In this paper, a stand-alone hybrid energy system consisting of wind, solar and diesel is proposed with the battery for energy storage. Wind and Solar is the primary power source of the system to take full advantage of renewable energy, diesel may be used as a backup system.

The proposed Wind, Solar and Diesel Hybrid system is shown in Fig 1.

2.1 Wind Power Generation System (WPGS)

In order to achieve the maximum power point in the wind power generation system, it is necessary to install the Power Electronic Converters between the Wind Turbine Generator (WTG) and the Grid [17]. The function of the wind turbine is to convert kinetic energy in to mechanical energy which is given to the generator.
The mechanical power output of Generator is expressed as

$$P_m = \frac{1}{2}\rho A V_\omega^2 C_p(\beta,\lambda) \qquad (1)$$

where ρ is the air density, A is the area swept by blades, $V\omega$ is the wind velocity in m/s, and Cp is power

coefficient. It is the function of blade pitch angle β and tip speed ratio λ. Tip speed ratio is defined by

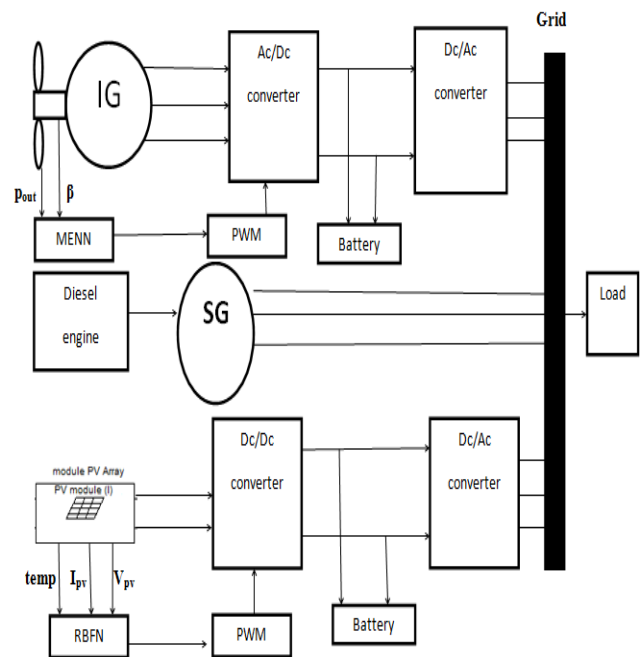$$\lambda = \frac{\omega_r}{V_\omega} \qquad (2)$$

Fig 1: Proposed Block Diagram

where r is the wind turbine blade radius, and ω_r is the turbine speed. A variable-speed pitch-regulated wind turbine is considered in this paper, where the pitch angle controller plays an important role. Fig. 2 shows the groups of Cp–λ curves of the wind turbine used in this study at different pitch angles [17]. From the figure that Cp can be controlled by varying the pitch angle β. So the output power of the wind turbine can be adjusted by pitch angle control.

2.2 Photovoltaic Array

The PV array is constructed by many series or parallel connected solar cells [7]. Each solar cell is form by P-N junction semiconductor, which can produce currents by the photovoltaic effect. Parameters of solar cell Shown in Fig. 3, typical output power characteristic curves for the PV array under different insolation are shown in Fig. 4.

$$V_{PV} = \frac{nKT}{q} ln\left(\frac{I_{sc}}{I_{pv}} + 1\right) \qquad (3)$$

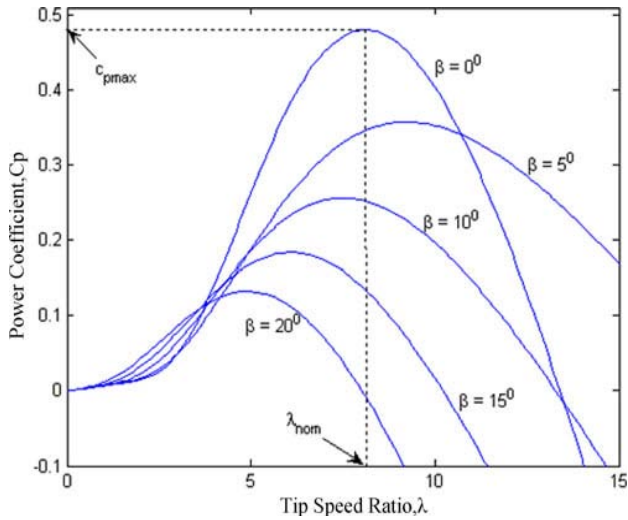$$I_{pv} = I_{sc} - I_{pvo}\left[\exp\left(\frac{q(V_{pv}+I_{pv}R_s)}{nKT}\right) - 1\right] - \frac{V_{pv}+R_sI_{sc}}{R_{sh}} \qquad (4)$$

Fig 2: *Cp –λ* characteristics of the WPGS at different pitch angles.

Fig 3: Equivalent Circuit of Solar Cell

this paper; the essential features can be described by the transfer function described in [2].

Fig 4: Output characteristics Curve of PV Array
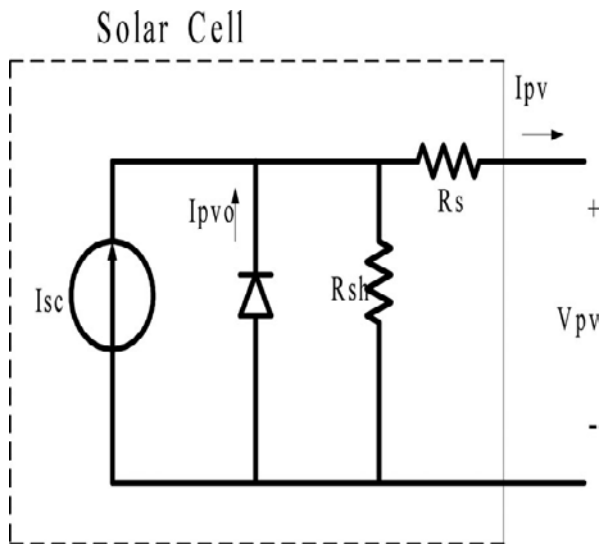

Fig 5: Fuel consumption Vs Power at various rotational speeds.

where R_s and R_{sh} are series and shunt resistances, respectively. I_{SC} is the light induced current, n is the ideality factor of p-n junction, I_{PVO} is the diode saturation current, K is Boltzmann constant ($8.63 \times 10{-}5$ J/∘K), and q is the electronic charge. I_{SC} depends on the irradiance level S and the array temperature T.

$$I_{sc} = I_{ref}[1 + ht(T_c - T_{ref})]\frac{S}{S_{ref}} \qquad (5)$$

where I_{ref} is the short-circuit current under the reference irradiance strength S_{ref} and temperature T_{ref}, ht is cell module temperature coefficient, while I_{PVO} depend on T only.

2.3 Diesel Engine System

The Diesel-generator Set (DGS) model comprises of combustion Chamber, Drive Train, and Synchronous Generator Models. A common Governor Model is used in
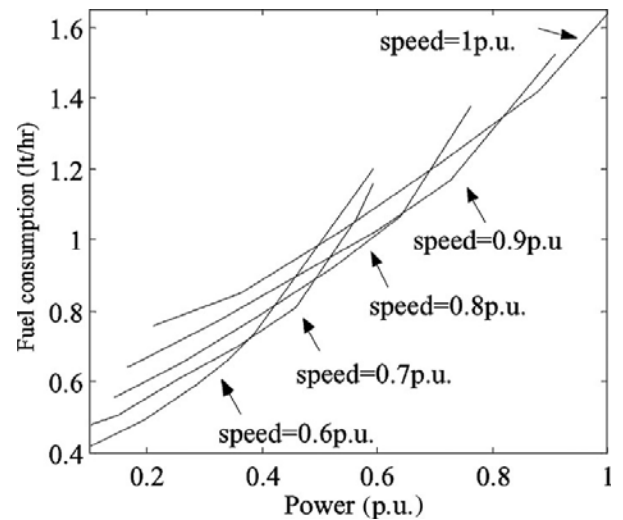
The fuel consumption of a diesel engine depends on the speed and torque of the machine. Fig. 5 shows the fuel consumption curves of a diesel engine for various rotational speeds. It can be seen that at 20% rated power, there is 50% fuel saving than that at 0.6 rated speeds. According to Fig. 5, a continuous function for the optimal operation Vs various speed can be formed tangent to all the curves. In order to minimize the fuel consumption, the speed demand (optimum speed) for the diesel engine is calculated by building up a look-up table where the optimal power-speed curve is implemented.

2.3 Battery Energy Storage System (BESS)

The battery load current rapidly changes according to changes in weather conditions and power command for the bus inverter in operation. The DC-bus voltage will be regulated to stay within a stable region regardless of the battery-current variation. When the DC bus voltage V_{dc}

becomes larger than the upper limit V_{dc} up, charging mode begins with the voltage command $V*_{dc}$ equal to the upper limit and continues until the DC voltage reaches the limit. If V_{dc} goes below the lower limit V_{dc} low, then the voltage target is bounded at the lower limit and the converter starts operating in boost mode.
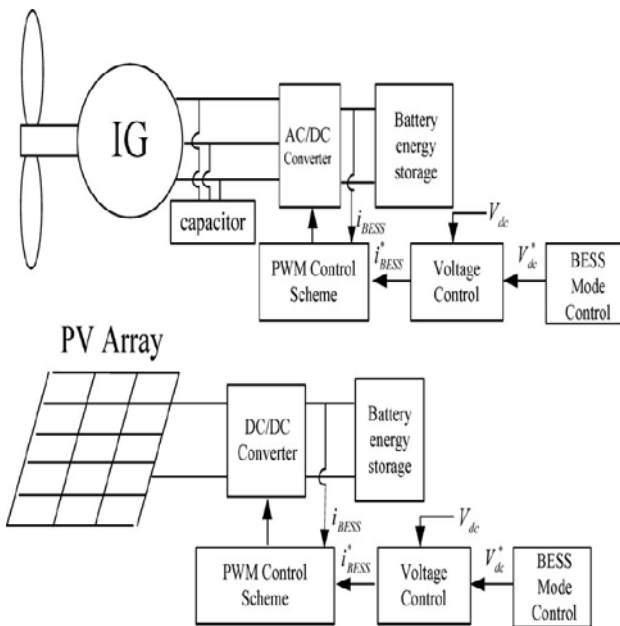

Fig 6: BESS structure with Interconnection diagram

3.   MPPT Control Algorithm for WPGS

3.1 Design of Modified Elman Neural Network

Architecture of an ENN including the input layer, the hidden layer, the context layer, and output layer which is shown in Fig.7 , Modified ENN also similar to ENN which has the major difference multiplied by its coefficient α ranging as $(0 \leq \alpha < 1)$ shown in Fig .8,In proposed system the MENN has two inputs where the control law is defined as $i*_q$, and the ENN inputs are $e^{(1)}_1$ and $e^{(1)}_2$ with, $e^{(1)}_1 = P_{ref} - P_{out}$ and $e^{(1)}_2 = \beta_c - \beta$ in this paper.

The proposed MENN [14, 18] takes the feedback into account, and a better learning efficiency can be obtained. Moreover, to make the neurons sensitive to the history of input data, self connections of the context nodes and output feedback node are added. So, the proposed MENN combines the ability of dealing with nonlinear problems, can effectively improve the convergence precision and reduce learning time.
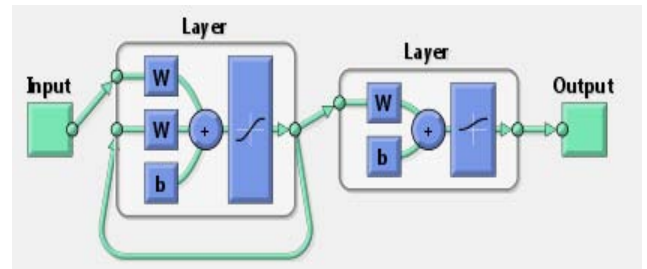

Fig 7: Simple Elman Neural Network.

The basic functions of each layer are as follow

Layer 1: **Input Layer**

In the input layer, the node is defined by

$$\text{net}^{(1)}_i = e^{(1)}_i (k) \qquad (6)$$

$$x^{(1)}_i (k) = f^{(1)}_i(\text{net}^{(1)}_i (k)) = \text{net}^{(1)}_i \qquad (7)$$

where k represents the kth iteration, $e^{(1)}_i (k)$ and $x^{(1)}_i (k)$ are the input and the output of the layer, respectively.

Layer 2: **Hidden Layer**

In the hidden layer, the node is defined by

$$\text{net}^{(2)}_j = \sum_i (W_{ij} \times x^{(1)}_i (k)) + \sum_r (W_{rj} \times x^{(3)}_r (k)) \qquad (8)$$

$$x^{(2)}_j (k) = 1/1 + \exp(-\text{net}^{(2)}_j) \qquad (9)$$

where $x^{(1)}_i$ and $x^{(3)}_r$ are input and $x^{(2)}_j (k)$ is output of the hidden layer. $x^{(3)}_r (k)$ is also the output of the context layer, and W_{ij} and W_{rj} are the connecting weights of input neurons to hidden neurons and context neurons to hidden neurons, respectively.

Layer 3: **Context Layer**

In the context layer, the node input and output are represented as,

$$x^{(3)}_r (k) = \alpha\, x^{(3)}_r (k - 1) + x^{(2)}_j (k - 1) \qquad (10)$$

where $0 \leq \alpha < 1$ is the self-connecting feedback gain.

Layer 4: **Output Layer**

In the output layer, the node input and output are represented as

$$\text{net}^{(4)}_o (k) = \Sigma_j W_{jo} \times x^{(2)}_j (k) \qquad (11)$$

$$y^{(4)}_o (k) = f^{(4)}_o (\text{net}^{(4)}_o (k)) = \text{net}^{(4)}_o (k) = i*_q \qquad (12)$$

where W_{jo} is the connecting weight of hidden neurons to output neurons, and $y^{(4)}_o (k)$ is the output of the MENN

and also the control effort of the proposed controller.

Once the MENN has been initialized, a supervised learning is used to train this system based on gradient descent. The derivation is the same as that of the back-propagation algorithm [14,18]. It is employed to adjust the parameters W_{jo}, Wrj, and W_{ij} of the MENN by using the training patterns. By recursive application of the chain rule, the error term for each layer is calculated, and updated. Supervised learning is to minimize the error function E expressed as

$$E = 1/2 \ (P_{\text{out}} - P_{\text{ref}})^2 = 1/2 \ e^2 \qquad (13)$$

where P_{out} and P_{ref} represent the actual output power and the reference output power of the generator, respectively, and e denotes the tracking error. A common supervised training algorithm is used in this paper, the essential features can be seen in[14] and [18].
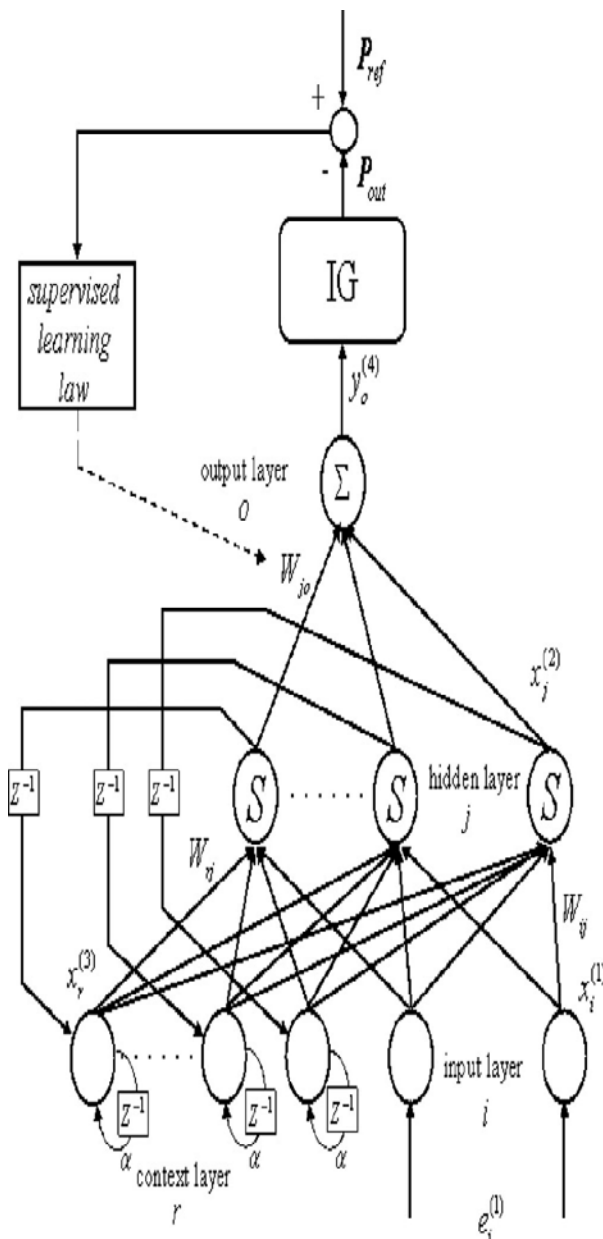

Fig 8: Structure of Modified Elman Neural Network

4. MPPT Control Algorithm for PV System

The proposed PV system is composed of solar panels, a dc/dc converter, battery storage, a dc/ac inverter, and a control algorithm, generally performed by a microcontroller to track the maximum power continuously. MPPT is also used to provide a constant voltage to the required load.

4.1 Design of Radial Bias Function Network

Radial Bias Function Network are embedded in to a two layer feed forward network [16]. Such a network is characterized by a set of inputs and set of outputs. In between the two layers are called hidden layer. In the proposed RBFN, the number of units in the input, hidden, and output layers are three, nine, and one, respectively. In order to apply RBFN control, PV system in Fig. 9 is linearized in this section. The PWM module is used to generate PWM pulses to control the duty cycle of the switch. The inputs of three layer RBFN is $X^1_1 = V_{pv}$,$X^1_2 = I_{pv}$ and $X^1_3 =$ Temperature.

Basic Nodes Operation:

Layer 1: Input Layer

The nodes in this layer are used to directly transmit the numerical inputs to the next layer. The net input and output are represented as

$$\text{net}^{(1)}_i = x^{(1)}_i \ (N) \qquad (14)$$

$$y^{(1)}_i \ (N) = f^{(1)}_i(\text{net}^{(1)}_i \ (N)) = \text{net}^{(1)}_i \ (N), \ i = 1, \ 2 \quad (15)$$

Layer 2: Hidden Layer

Every node performs a Gaussian function. The Gaussian function, a particular example of radial basic functions, is used here as a membership function. Then

$$\text{net}^{(2)}_j \ (N) = -(X - M_j)^T \sum_j (X - Mj) \qquad (16)$$

$$y^{(2)}_j \ (N) = f^{(2)}j(\text{net}^{(2)}_j \ (N)) = \exp(\text{net}^{(2)}_j \ (N)) \ \ j = 1,.9 \quad (17)$$

Layer 3: Output Layer

The single node k in this layer is denoted by Σ, which computes the overall output as the summation of all incoming signals by

$$\text{net}^{(3)}_k = \sum_j w_j \ y^{(2)}_j \ (N) \qquad (18)$$

$$y^{(3)}_k \ (N) = f^{(3)}_k \ (\text{net}^{(3)}_k \ (N) = \text{net}^{(3)}_k \ (N) \qquad (19)$$

where w_j is the connective weight between the hidden and the output layers.

4.2 Supervised Learning Process

Once the RBFN has been initialized, a supervised learning law of gradient descent is used to train this system. The derivation is the same as that of the back-propagation

algorithm. It is employed to adjust the parameters m_{ij}, σ_{ij}, and w_j of the RBFN by using the training patterns. By recursive application of the chain rule, the error term for each layer is calculated, and updated. The adjustment of the parameters for learning and the weight of links enhance the performance of solar systems. The purpose of supervised learning is to minimize the error function E expressed as

$$E = 1/2 \ (V_{dc} - V_{MPPT})^2 \qquad (20)$$

where V_{dc} and V_{MPPT} represent the reference output voltage and the actual output voltage. A common supervised training algorithm is used in this paper.

4.3 Harmonic Analysis

Harmonic currents make main issues in grid part. It poses a challenge in the measurement of power quality. It requires great accuracy, even for higher frequencies, since the measurement refers to interharmonics that are in the range of 0.1% of the rated current. In the proposed system
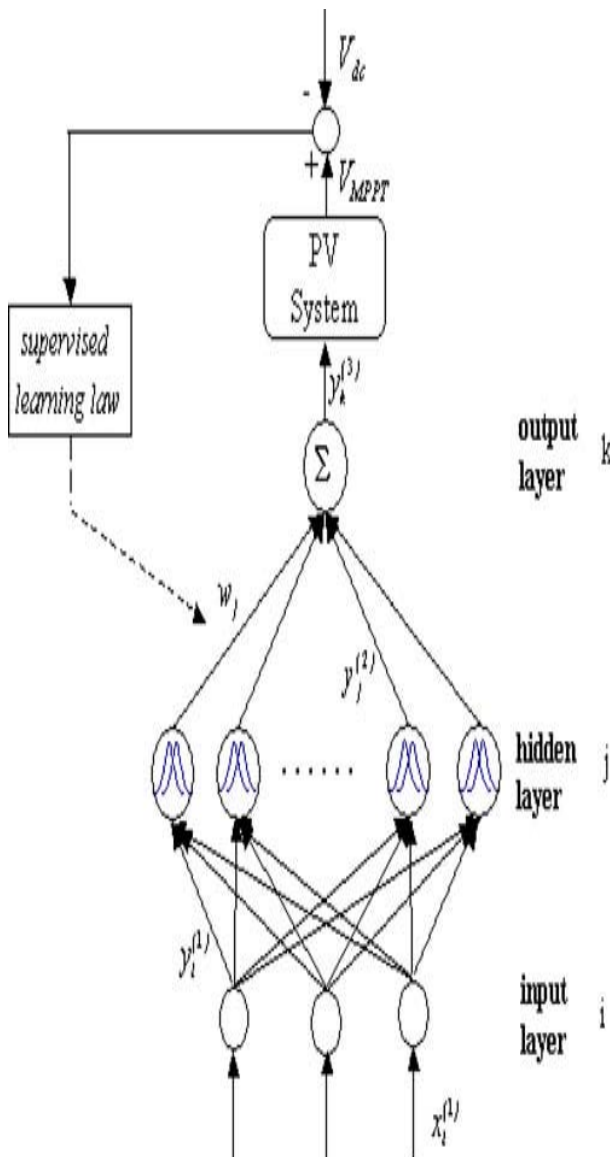

Fig 9: Radial Bias Function Network

the Total Harmonic Distortion(THD) is measured by the Matlab/Simulink. It should be generally less than 1.48% in the grid.

With regard to high-order harmonics, EN 50160 standards does not specify any limits but states that high-order harmonics are usually negligible, though fairly unpredictable. Therefore THD = 4.61% for nominal phase-to-phase voltage.

5. Simulation Diagram and Results

The proposed system comprises of an 3 phase Induction Generator, PV array, Diesel Generator, a current control PWM Ac/Dc converter, a Field-Orientation Mechanism including the Coordinate Translator, a Current Controlled Dc/Ac inverter, and the MPPT controller, where the MENN and RBFN were applied in this paper. The Dc-bus voltage is regulated at a constant value so the real power from the wind turbine and PV system will pass to the grid. By using the Reference Frame Theory and the linearization technique, the hybrid power generation system can be represented by the Matlab 2009/Simulink as shown in Fig. 10.

The below Table 1,2,3, 4 and 5 represents the Wind Induction Generator Parameters, Photovoltaic Array Parameter, Diesel Synchronous Generator Parameters, Battery Energy Storage Parameters, Load and Grid Parameters.

Simulation Parameters

Table 1: Wind Induction Generator

Rated Power (KW)	5
Voltage (V)	440
Frequency (HZ)	50
Inertia	0.6745
No of poles	4
Wind speed (M/S)	12

Table 2: Photovoltaic array

Maximum power in Module (KW)	1 KW/m^2
Module Number	4 x 4
Unit Rated Voltage(V)	24
Unit Rated current(I)	6.5
Irradiance Level (W/m^2)	800

Table 3: Diesel Synchronous Generator

Rated power (KW)	24
Voltage (V)	440
Frequency (HZ)	50
Inertia	0.75

No of poles	4

Table 4: Battery Energy Storage System & Load

Voltage (V)	220
Capacity (KWH)	15
Load (KW	40

Table 5: Grid

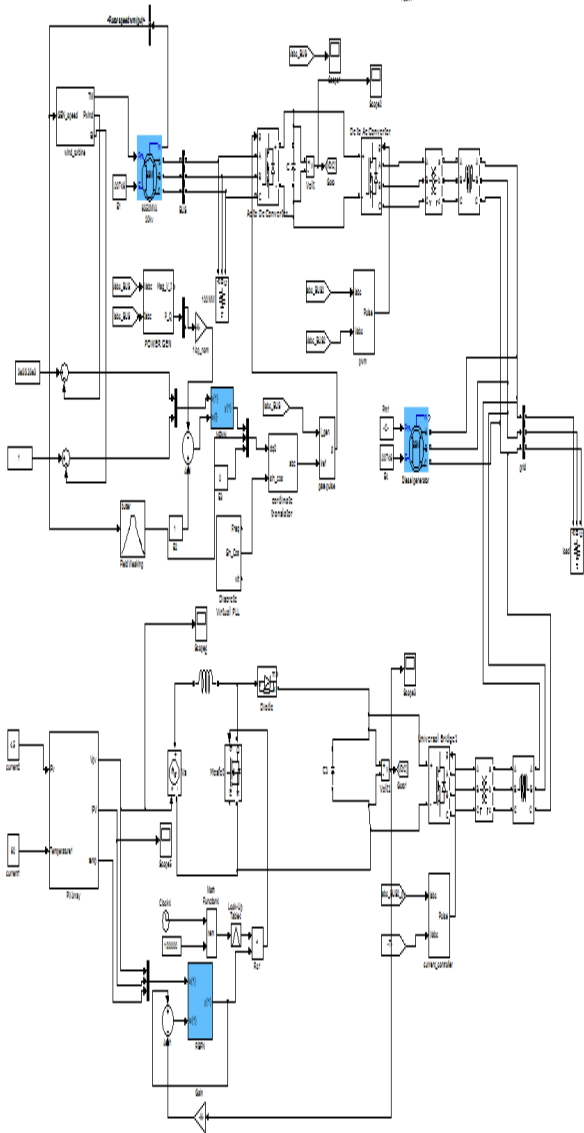| Voltage (V)	440
Frequency (HZ)	50
Phase	3

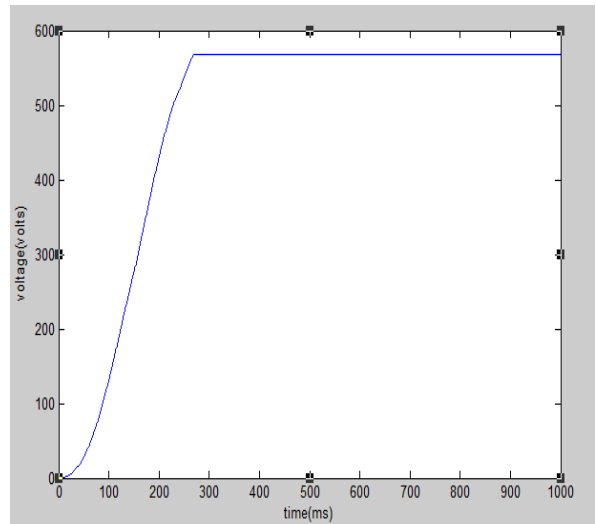Fig 10: Simulation Diagram for Hybrid Power Generation System

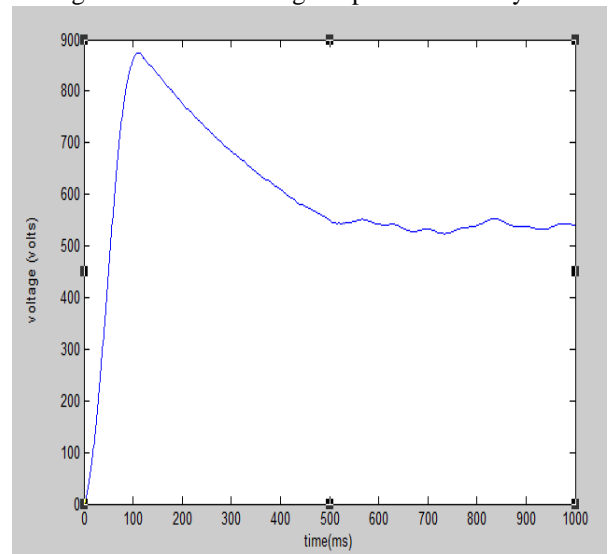Fig 11: MPPT Tracking Response of PV System
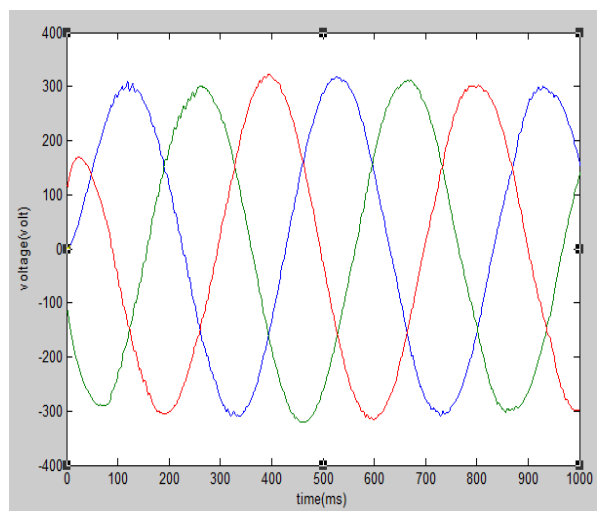

Fig 12: MPPT Tracking Response of WPGS

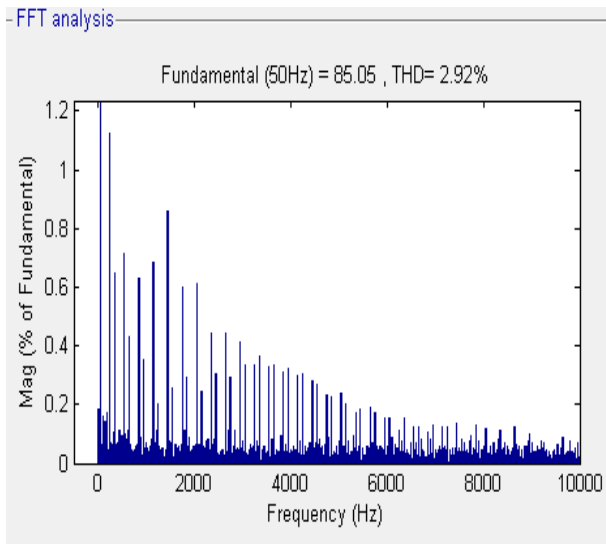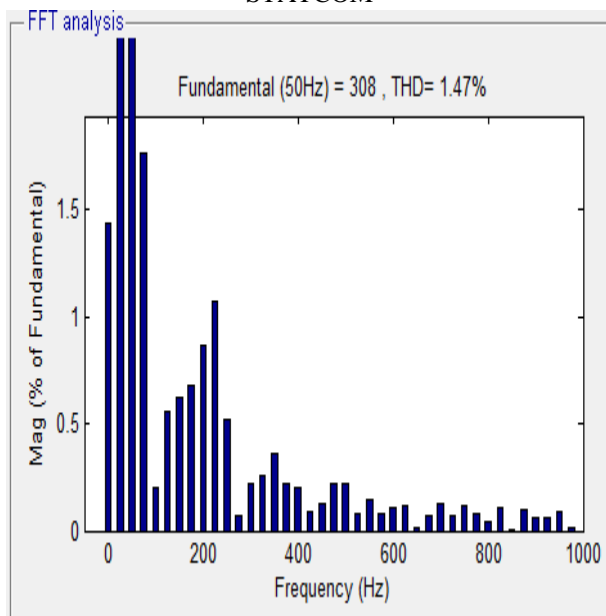Fig 13: Grid Voltage Under Sudden Load Changes

Fig 14: FFT Analysis of Grid with PI controller based STATCOM

15: FFT Analysis of Grid with MENN and RBFN

Figure 11 and 12 shows the output when the MPPT is achieved under PV system and WPG. Figure 13 represent the constant Grid voltage output in hybrid power generation system under sudden load changes. Figure 14 and 15 shows the output compared with PI controller based STATCOM with THD 2.92% and in this proposed MENN and RBFN controller THD is reduced to 1.47% which gives better connected to load[19].

6. Conclusion

In this paper, a solar and wind - diesel hybrid power generation System was proposed and implemented. This Stand-Alone Hybrid Generation System can effectively extract the maximum power from the wind and PV system. Here the neural network controllers maintain THD below 1.48% in grid. An efficient power sharing technique among energy sources are successfully demonstrated with more efficiency, a better transient and more stability

response, even under disturbance conditions. The simulation model of the hybrid system was developed using MATLAB 2009/Simulink. The load frequency is regulated by the diesel generator by imposing the rotor currents with the slip frequency. The electrical torque of the WPGS generator is controlled to drive the system to the rotational speed where maximum energy can be captured. Depending on the load size and the power supplied by the WPGS generator, the control system regulates the DGS rotational speed to minimize the fuel consumption.

In future, any other source of renewable energy may be utilized in Hybrid Power Generation System and also the performance may be improved by minimising the THD. The Simulations may also be carried out by using any other software such as Proteus, Multisim etc.

References

[1] G. Abad, M. A. Rodriguez, G. Iwanski, and J. Poza, "Direct power control of doubly-fed-induction-generator-based wind turbine under unbalanced grid voltage," *IEEE Trans. Power Electron.*, vol. 25, no. 2, pp. 442–452, Feb. 2010.
[2] A. J. Rudell, J. A. M. Bleijs, L. Freris, D. G. Infield, and G. A. Smith, "A wind diesel system with variable speed flywheel storage," *Wind Eng.*, vol. 17, pp. 129–145, May 1993.
[3] Z. Chen and Y. Hu, "A hybrid generation system using variable speed wind turbines and diesel units," in *Proc. IEEE Ind. Electron. Soc. Annu. Meeting Conf.*, pp. 2729–2734, Nov. 2003.
[4] M. Tolbet and W.A. Peterson "Gen Sets" IEEE- April - 2003.
[5] B. S. Borowy and Z. M. Salameh, "Dynamic response to a stand-alone wind energy conversion system with battery energy storage to a wind gust," *IEEE Trans. Energy Convers.*, vol. 12, no. 1, pp. 73–78, Mar. 1997.
[6] N. Femia, G. Petrone, G. Spagnuolo, and M. Vitelli, "Optimization of perturb and observe maximum power point tracking method," *IEEE Trans. Power Electron.*, vol. 20, no. 4, pp. 963–739, Jul. 2005.
[7] B. Yang, Y. Zhao, and X. He, "Design and analysis of a grid-connected photovoltaic power system," *IEEE Trans. Power Electron.*, vol. 25, no. 4, pp. 992–1000, Apr. 2010.
[8] Joanne Hui, Alireza Bakhshai, and Praveen K. Jain, " A Hybrid Wind-Solar Energy System: A New Rectifier Stage Topology" *IEEE Trans, Jun* 2010.
[9] B. S. Borowy and Z. M. Salameh, "Dynamic response to a stand-alone wind energy conversion system with battery energy storage to a wind gust," *IEEE Trans. Energy Convers.*, vol. 12, no. 1, pp. 73–78, Mar. 1997.
[10] B. S. Borowy and Z. M. Salameh, "Methodology for optimally sizing the combination of a battery bank and PV array in a wind/PV hybrid system," *IEEE Trans. Energy Conv.*, vol. 11, no. 2, pp. 367–375, Jun. 1996.
[11] Ramana. A and Chinnakullay Reddy. D, "Constant power control of DFIG wind turbines with super capacitor

energy storage." IJEI, vol 1, issue 6, pp no 32-39, Oct 2012.

[12] N. Prakash and K. Sankar, " Neural Network-Control Scheme for Grid Connected Hybrid Power Generation System for Power Quality Improvement" *IOSR-JEEE., vol 3, issue 1,pp. 53-59, Nov. 2012*.

[13] E. Muljadi and C. P. Butterfield, "Pitch-controlled variable-speed wind turbine generation," *IEEE Trans. Ind. Appl.*, vol. 37, no. 1, pp. 240–246, Jan./Feb. 2001.

[14] F. J. Lin and Y. C. Hung, "FPGA based Elman neural network control system for linear ultrasonic motor," *IEEE Trans. Ferr.Ultras. And Freq. Control.*, vol. 56, no. 1, pp. 101–113, Jan. 2009.

[15] Y. M. Cheng, Y. C. Liu, S. C. Hung, and C. S. Cheng, "Multi-input inverter for grid-connected hybrid PV/wind power system," *IEEE Trans. Power Electron.*, vol. 22, no. 3, pp. 1070–1076, May 2007.

[16] S. Seshagiri and H. K. Khail, "Output feedback control of nonlinear systems using RBF neural networks," *IEEE Trans. Neural Network.*, vol. 11, no. 1, pp. 69–79, Jan. 2000.

[17] W. Sharad Mohod, *Member, IEEE,* and Mohan V. Aware "Micro wind power generation with battery energy storage for critical load" IEEE Systems Journal, vol. 6, no. 1, March 2012.

[18] H. Liu, S. Wang, and P. Ouyang, "Fault diagnosis based on improved Elman neural network for a hydraulic servo system," in *Proc. Int. Conf. 1Robot., Autom. Mechatronics*, pp no 1-6, Dec. 2006.

[19] Sharad w. Mohod, Mohan V. Aware," A STATCOM-control scheme for grid connected wind energy system for power quality improvement", IEEE power systems journal, vol. 4, no. 3, Sept 2010.

Authors Profile

N.Prakash received his B.E degree in Electrical and Electronics Engineering from Roever Engineering College in 2011 and pursuing his M.E. Power System Engineering from Adhiyamaan College of Engineering, at Hosur, India. His area of interest is power quality and power systems.

R.Ravikumar received his B.E degree in Electrical and Electronics Engineering from Adhiyamaan College of Engineering in 2000, Master of Engineering degree in Power Electronics and drives from Government College of Engineering, Bargur in 2005. He is currently pursuing Ph.D in Anna University Chennai and his area of interest is Power Electronics. He is now Professor in Electrical and Electronics Engineering, Adhiyamaan College of Engineering, Hosur, India.

I.Gnanambal received her B.E degree in Electrical and Electronics Engineering from university of madras in 1981, Master of Engineering degree from Government College of Technology, Coimbatore in 2005. She received Ph.D in Anna University Chennai. Currently, she is Head & Professor in Electrical and Electronics Engineering, Government College of Engineering, Salem, India.